

## Diagnostic Accuracy of Contrast-Enhanced MRI in Detection of Ovarian Malignant Masses

Piriha Nisar\*, Varsha, Abdul Samad, Shaista Shoukat, Sumera Shahbaz, Sanjana

Department of Radiology, Jinnah Postgraduate Medical Centre, Karachi, Pakistan

\*Corresponding author's email address: [pirahnisar9197@gmail.com](mailto:pirahnisar9197@gmail.com)

(Received, 24<sup>th</sup> April 2025, Accepted 22<sup>nd</sup> June 2025, Published 30<sup>th</sup> June 2025)

**Abstract:** Characterizing indeterminate adnexal masses remains a clinical challenge. Contrast-enhanced MRI (CE-MRI) may enhance the discrimination between benign and malignant ovarian lesions, thereby refining surgical triage. **Objective:** To determine the diagnostic accuracy of CE-MRI for detecting ovarian malignancy using histopathology as the reference standard. **Methods:** We conducted an observational study over six months, commencing from June 2024 to December 2024, at a tertiary referral center (Department of Radiology, JPMC, Karachi). Consecutive women ( $\geq 18$  years) with suspected ovarian masses underwent standardized pelvic CE-MRI (multiparametric protocol with dynamic contrast enhancement). Imaging features (size, shape, septations/solid components, enhancement pattern, necrosis) and an overall CE-MRI impression (benign vs malignant) were recorded. All patients proceeded to definitive surgery; histopathology (malignant vs benign, subtype, grade) served as the Gold standard. Diagnostic performance metrics (sensitivity, specificity, PPV, NPV, accuracy) were calculated from  $2 \times 2$  tables; ROC analysis quantified discrimination. **Results:** A total of 152 women were included (mean age  $47.05 \pm 11.28$  years; symptom duration  $8.69 \pm 4.11$  weeks). Mean lesion size was  $8.54 \pm 3.31$  cm on baseline imaging and  $7.93 \pm 3.12$  cm on CE-MRI. CE-MRI impressions were malignant in 75 (49.3%) cases; histopathology confirmed malignancy in 73 (48.0%). The  $2 \times 2$  table yielded 66 true positives, nine false positives, 70 true negatives, and seven false negatives. CE-MRI demonstrated sensitivity 90.4%, specificity 88.6%, PPV 88.0%, NPV 90.9%, and overall accuracy 89.5%. ROC analysis showed strong discrimination (AUC 0.895,  $p < 0.0001$ ). **Conclusion:** In a real-world referral cohort, CE-MRI demonstrated high diagnostic accuracy in differentiating malignant from benign ovarian masses, with excellent sensitivity and specificity, and an AUC approaching 0.90. CE-MRI thus provides robust second-line problem-solving after initial imaging and supports informed surgical planning.

**Keywords:** Ovarian neoplasms; Adnexal mass; Magnetic resonance imaging; Contrast-enhanced MRI; Diagnostic accuracy; Sensitivity and specificity; Receiver operating characteristic (ROC); Histopathology; O-RADS MRI; Diffusion-weighted imaging (DWI)

**[How to Cite:** Nisar P, Varsha, Samad A, Shoukat S, Shahbaz S, Sanjana. Diagnostic accuracy of contrast-enhanced MRI in the detection of ovarian malignant masses. *Biol. Clin. Sci. Res. J.*, 2025; 6(6): 407-410. doi: <https://doi.org/10.54112/bcsrj.v6i6.1972>

### Introduction

Ovarian cancer remains a leading cause of gynecologic cancer mortality worldwide, with 324,603 new cases and 206,956 deaths estimated in 2022, largely due to late-stage presentation and limitations of first-line imaging to confidently characterize indeterminate adnexal masses (1). Standardized MRI lexicons and risk scores were developed to reduce variability and improve benign–malignant discrimination, notably the O-RADS MRI lexicon and scoring system (2).

In a landmark multicenter cohort of 1,340 women with sonographically indeterminate masses, the O-RADS MRI score demonstrated a sensitivity of 0.93 and specificity of 0.91, with an AUC of 0.961 and good interreader agreement, supporting its clinical adoption to curtail unnecessary surgery while maintaining cancer detection (3). A 2023 systematic review and meta-analysis further reported category-wise malignancy rates of approximately 0.1% (O-RADS 2), 6% (3), 60% (4), and 96% (5), facilitating pretest–posttest decision-making (4). An updated 2024 meta-analysis that accounted for selection bias estimated a pooled sensitivity of ~93% (low-bias studies) and specificity of ~90%, highlighting a strong rule-out capability and moderate rule-in performance (5).

Technically, dynamic contrast–enhanced MRI (DCE-MRI) and diffusion-weighted imaging (DWI) provide complementary information on vascular and microstructural aspects. A meta-analysis of DCE-MRI reported a pooled sensitivity of 88% and a specificity of 93% for quantitative analyses and 85%/85% for semi-quantitative approaches in diagnosing malignant ovarian tumors (6). DWI meta-analyses similarly show high pooled performance, with a sensitivity ~of approximately 0.93 and a specificity ~of roughly 0.89 for benign–malignant discrimination (7). Synthesizing across modalities and scoring systems, reviews suggest

that MRI outperforms CT for characterizing ovarian tumors and assessing peritoneal disease, providing higher sensitivity and specificity, as well as more actionable risk stratification to guide management (4, 5).

Notably, even unenhanced MRI protocols have recently demonstrated promising accuracy in indeterminate masses, with sensitivities ranging from 86% to 98%, specificities ranging from 86% to 98%, and an overall accuracy of ~94%, supporting a role when gadolinium is contraindicated or unavailable (8). Together, these data underscore that contrast-enhanced, multiparametric MRI, ideally interpreted with a standardized system such as O-RADS, offers high diagnostic accuracy, improves triage, and may reduce unnecessary surgery compared with conventional pathways (2–6, 8–10).

**Objective:** To determine the diagnostic accuracy (sensitivity, specificity, PPV, NPV) of contrast-enhanced MRI for detecting ovarian malignant masses using histopathology as the Gold standard, and to compare accuracy against conventional imaging modalities.

### Methodology

We conducted an observational study in the Department of Radiology at JPMC, Karachi, over six months, following approval by the ethics committee. A non-probability consecutive sample of 152 women ( $\geq 18$  years) with suspected ovarian masses on clinical assessment and/or initial imaging (US, CT, or MRI) was enrolled after written informed consent. We excluded patients  $< 18$  years, pregnant women, those with prior hypersensitivity to gadolinium or other contraindications to MRI, and unstable medical conditions.

All eligible participants underwent contrast-enhanced pelvic MRI using the institution's standardized female pelvis protocol. Gadolinium-based



contrast was administered intravenously; sequences included multiplanar T1- and T2-weighted imaging, dynamic contrast enhancement, and routine diffusion-weighted imaging sequences, as per local practice. MRI reports recorded lesion size, shape, septations/solid components, enhancement pattern, necrosis, and an overall CE-MRI impression (benign vs. malignant), where available. Standardized scoring terminology (e.g., O-RADS lexicon) was used for consistency.

Subsequently, patients underwent definitive surgery (cystectomy, oophorectomy, or TAH+BSO) per clinical indications. Histopathology served as the reference standard, documenting Diagnosis (benign, borderline, or malignant), histologic subtype, grade, and metastasis. Trained staff extracted demographics, symptoms, duration, prior history, initial modality findings, CE-MRI features/impression, operative details, and histopathology to a secure database.

Statistical analysis (planned in SPSS v21) was used to summarize demographics and imaging characteristics. Diagnostic accuracy of CE-MRI versus histopathology was calculated (sensitivity, specificity, PPV, NPV, and 95% CIs (from 2x2 tables; ROC analysis explored thresholds for technical parameters when applicable. Comparisons with conventional imaging (US/CT) were assessed where both tests were available.  $p < 0.05$  was considered significant.

## Results

Among 152 women, the mean age was  $47.05 \pm 11.28$  years, and symptoms had been present for  $8.69 \pm 4.11$  weeks. The most common presenting complaint was abdominal pain in 59 (39%) of patients, followed by bloating in 42 (28%), abnormal bleeding in 24 (16%), incidental finding in 19 (13%), and weight loss in 8 (5%). A Prior ovarian mass history was reported in 40 (26.3%) cases. The baseline imaging mass size measured  $8.54 \pm 3.31$  cm, while the CE-MRI size was  $7.93 \pm 3.12$  cm (Table 1).

Regarding tumor-related variables, the initial imaging modality was ultrasound in 104 cases (68.4%), CT in 31 cases (20.4%), and MRI in 17 cases (11.2%). Baseline shape was oval in 62 (40.8 %), irregular in 53 (34.9 %), and round in 37 (24.3 %) septations were present in 60 (39.5 %), a solid component in 64 (42.1 %), and vascularity was moderate in 64 (42.1 %), low in 54 (35.5 %), and high in 34 (22.4 %). On CE-MRI, the shape was oval in 69 (45.4 %), irregular in 46 (30.3 %), and round in 37 (24.3 %); the enhancement pattern was progressive in 64 (42.1 %), plateau in 50 (32.9 %), and washout in 38 (25.0 %); necrosis was seen in 32 (21.1 %). The overall CE-MRI impression was benign in 77 cases (50.7%) and malignant in 75 cases (49.3%). Histopathology confirmed malignancy in 73 (48.0%) cases, with types distributed as: high-grade serous carcinoma 39 (25.7%), endometrioid carcinoma 13 (8.6%), mucinous carcinoma 10 (6.6%), clear cell carcinoma 2 (1.3%), borderline tumor 5 (3.3%), and other epithelial 4 (2.6%); benign diagnoses included

endometrioma 25 (16.4%), mucinous cystadenoma 16 (10.5%), serous cystadenoma 16 (10.5%), fibroma/thecoma 14 (9.2%), mature cystic teratoma 5 (3.3%), and other benign 3 (2.0%). Histological grade was high in 54 (35.5 %), low in 19 (12.5 %), and not applicable/benign in 79 (52.0 %); metastasis was present in 14 (9.2 %). Surgical management included TAH+BSO in 52 (34.2 %), cystectomy in 51 (33.6 %), and unilateral salpingo-oophorectomy in 49 (32.2 %) (Table 2).

For diagnostic performance, the cross-tabulation of CE-MRI impressions against histopathology revealed 66 true positives, nine false positives, 70 true negatives, and seven false negatives (total  $n = 152$ ). This yielded a sensitivity of 90.4%, a specificity of 88.6%, a positive predictive value of 88.0%, a negative predictive value of 90.9%, and an overall accuracy of 89.5% (Table 3). ROC analysis demonstrated strong discrimination with an AUC of 0.895 and  $p < 0.0001$  (Figure 1).

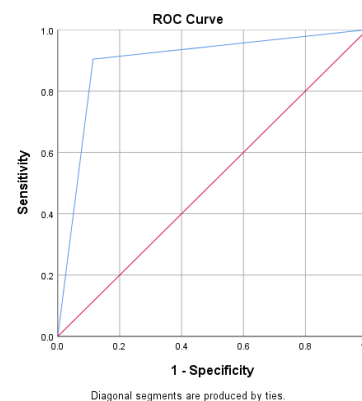


**Figure 1: ROC curve analysis with an AUC value of 0.895 and  $p < 0.0001$**

**Table 1: Demographic and clinical variables**

| variable                     | Mean and frequency |
|------------------------------|--------------------|
| Age (years)                  | 47.05±11.28        |
| Duration of symptoms (weeks) | 8.69±4.11          |
| Presenting symptom           |                    |
| Abdominal pain               | 59 (39 %)          |
| Abnormal bleeding            | 24 (16 %)          |
| Bloating                     | 42 (28 %)          |
| Incidental finding           | 19 (13 %)          |
| Weight loss                  | 8 (5 %)            |
| Prior ovarian mass history   | 40 (26.3 %)        |
| Baseline imaging size (cm)   | 8.54±3.31          |
| CE-MRI size (cm)             | 7.93±3.12          |

**Table 2: Tumor variables**

| variable                          | category   | frequency | percentage |
|-----------------------------------|------------|-----------|------------|
| Initial imaging modality          | CT         | 31        | 20.4       |
|                                   | MRI        | 17        | 11.2       |
|                                   | Ultrasound | 104       | 68.4       |
| Baseline imaging: shape           | Irregular  | 53        | 34.9       |
|                                   | Oval       | 62        | 40.8       |
|                                   | Round      | 37        | 24.3       |
| Baseline imaging: septations      | Yes        | 60        | 39.5       |
| Baseline imaging: solid component | Yes        | 64        | 42.1       |
| Baseline imaging: vascularity     | High       | 34        | 22.4       |
|                                   | Low        | 54        | 35.5       |
|                                   | Moderate   | 64        | 42.1       |
| CE-MRI: shape                     | Irregular  | 46        | 30.3       |
|                                   | Oval       | 69        | 45.4       |
|                                   | Round      | 37        | 24.3       |

|                             |                                  |    |      |
|-----------------------------|----------------------------------|----|------|
| CE-MRI: enhancement pattern | Plateau                          | 50 | 32.9 |
|                             | Progressive                      | 64 | 42.1 |
|                             | Washout                          | 38 | 25   |
| CE-MRI: necrosis            | Yes                              | 32 | 21.1 |
| CE-MRI overall impression   | Benign                           | 77 | 50.7 |
|                             | Malignant                        | 75 | 49.3 |
| Histopathology: malignant   | Yes                              | 73 | 48   |
| Histopathology: type        | Borderline tumor                 | 5  | 3.3  |
|                             | Clear cell carcinoma             | 2  | 1.3  |
|                             | Endometrioid carcinoma           | 13 | 8.6  |
|                             | Endometrioma                     | 25 | 16.4 |
|                             | Fibroma/Thecoma                  | 14 | 9.2  |
|                             | High-grade serous carcinoma      | 39 | 25.7 |
|                             | Mature cystic teratoma           | 5  | 3.3  |
|                             | Mucinous carcinoma               | 10 | 6.6  |
|                             | Mucinous cystadenoma             | 16 | 10.5 |
|                             | Other benign                     | 3  | 2    |
|                             | Other epithelial                 | 4  | 2.6  |
|                             | Serous cystadenoma               | 16 | 10.5 |
| Histological grade          | High                             | 54 | 35.5 |
|                             | Low                              | 19 | 12.5 |
|                             | nan                              | 79 | 52   |
| Metastasis                  | Yes                              | 14 | 9.2  |
| Surgery type                | Cystectomy                       | 51 | 33.6 |
|                             | TAH+BSO                          | 52 | 34.2 |
|                             | Unilateral salpingo-oophorectomy | 49 | 32.2 |

**Table 3: Accuracy variables**

| Variables    | Histopathology Positive | Histopathology Negative | Row Total |
|--------------|-------------------------|-------------------------|-----------|
| MRI Positive | 66                      | 9                       | 75        |
| MRI Negative | 7                       | 70                      | 77        |
| Total        | 73                      | 79                      | 152       |
| Sensitivity  | 90.4%                   |                         |           |
| Specificity  | 88.6%                   |                         |           |
| PPV          | 88.0%                   |                         |           |
| NPV          | 90.9%                   |                         |           |
| Accuracy     | 89.5%                   |                         |           |

## Discussion

Our study demonstrated the high diagnostic performance of CE-MRI for malignant ovarian masses, with a sensitivity of 90.4%, a specificity of 88.6%, an accuracy of 89.5%, and an AUC of 0.895, which aligns closely with classic MR literature reporting overall accuracies of approximately 91–93% and excellent reader agreement for adnexal mass characterization. Hricak et al. reported **93% accuracy** in a prospective multivariate analysis, with enhancement and necrosis among the strongest predictors of malignancy—patterns that we also observed as drivers of positive CE-MRI impressions (11). Similar accuracies (~91%) were shown by Sohaib et al. and Saini et al., supporting the external plausibility of our operating characteristics despite differences in scanners, protocols, and case mix (12,13).

Beyond point estimates, our AUC of 0.895 is consistent with MR's established role as a problem-solving modality after indeterminate ultrasound (US). In a meta-analysis and Bayesian framework, Kinkel et al. demonstrated that when US is indeterminate, a second-line MR examination shifts post-test probabilities more effectively than CT or repeat Doppler US in both pre- and postmenopausal women, supporting the clinical utility of CE-MRI, where management hinges on ruling in/out malignancy (14). Consolidating multiparametric MR features within structured interpretations further improves triage in routine practice, as emphasized by contemporary multimodality reviews (15).

Functional sequences likely underpinned our performance. Reviews highlight that DWI and perfusion (DCE-MRI) add microstructural and

vascular cues that complement morphology and enhancement timing, improving benign–malignant discrimination and reader confidence (16). The incorporation of ADC metrics has been shown to re-stratify lesions within MR risk frameworks, reducing equivocal categories and increasing the proportion of correctly identified high-risk masses, an effect directionally consistent with our relatively low false-negative rate (7/73) (17).

When compared with advanced US-based risk models, our CE-MRI results are slightly lower than the very high AUCs reported for IOTA-ADNEX in specialist hands (e.g., AUC ~0.95 for benign vs. malignant in the original BMJ report). However, meta-validation across diverse settings shows performance attenuation and underscores the continued need for second-line MR in indeterminate or complex lesions, precisely the niche of our cohort (18, 19). The complementarity of high-quality US risk modeling and MR problem-solving is therefore pragmatic rather than competitive.

Our false positives (n = 9) were clinically acceptable. They may, in part, reflect borderline tumors, which are notorious mimics on imaging because papillary projections and septations can simulate invasive disease without stromal infiltration. Reviews of serous borderline ovarian tumors detail overlapping MRI appearances with carcinoma and variable enhancement behavior that can inflate MRI-based malignancy calls, findings that are concordant with our error profile and the distribution of histologies (borderline 3.3% (20).

Finally, the histologic spectrum in our series (predominance of high-grade serous carcinoma) mirrors the global epidemiology of epithelial ovarian

cancers, where serous histology is most common, lending face validity to our case mix and performance metrics in a real-world referral setting (21).

## Conclusion

Our findings reinforce CE-MRI as a robust diagnostic tool for characterizing adnexal masses, achieving accuracy metrics comparable to those of landmark MR studies and demonstrating strong discrimination in ROC analysis. Leveraging multiparametric MR (T2/T1, DCE, DWI/ADC) within standardized interpretive schemes can further reduce indeterminate outcomes, while borderline histotypes remain an expected and important source of false positivity. Integrating first-line US risk models with targeted second-line CE-MRI is a rational pathway to optimize triage and surgical planning.

## Declarations

### Data Availability statement

All data generated or analysed during the study are included in the manuscript.

### Ethics approval and consent to participate

Approved by the department concerned. (IRBEC-24)

### Consent for publication

Approved

### Funding

Not applicable

## Conflict of interest

The authors declared the absence of a conflict of interest.

## Author Contribution

PN (Resident)

Manuscript drafting, Study Design,

V (Resident)

Review of Literature, Data entry, Data analysis, and drafting an article.

AS (Resident)

Conception of Study, Development of Research Methodology Design,

SS (Head of Department of Radiology)

Study Design, manuscript review, and critical input.

SS (Associate Professor)

Manuscript drafting, Study Design,

S (Resident)

Review of Literature, Data entry, Data analysis, and drafting an article.

All authors reviewed the results and approved the final version of the manuscript. They are also accountable for the integrity of the study.

## References

1. Ferlay J, Ervik M, Lam F, et al. Global Cancer Observatory: Cancer Today—Ovary fact sheet (GLOBOCAN 2022). Lyon: IARC; 2024. Available from: <https://gco.iarc.who.int/today> (accessed 2025-09-24). [No DOI assigned]
2. Reinhold C, Rockall A, Sadowski EA, et al. Ovarian-Adnexal Reporting Lexicon for MRI: A White Paper of the ACR O-RADS MRI Committee. J Am Coll Radiol. 2021;18(5):713-729. <https://doi.org/10.1016/j.jacr.2020.12.022>
3. Thomassin-Naggara I, Poncelet E, Jalaguier-Coudray A, et al. O-RADS MRI score for risk stratification of sonographically indeterminate adnexal masses. JAMA Netw Open. 2020;3(1):e1919896. <https://doi.org/10.1001/jamanetworkopen.2019.19896>
4. Rizzo S, Cozzi A, Dolcianni M, et al. O-RADS MRI: Systematic review & meta-analysis of diagnostic performance and category-wise

- malignancy rates. Radiology. 2023;307(1):e220795. <https://doi.org/10.1148/radiol.220795>
5. Kılıçkap G, et al. Diagnostic performance of the O-RADS MRI system: systematic review, meta-analysis, and meta-regression. Diagn Interv Radiol. 2024. <https://doi.org/10.4274/dir.2024.242784>
6. Wei M, Bo F, Cao H, et al. Diagnostic performance of DCE-MRI for malignant ovarian tumors: systematic review and meta-analysis. Acta Radiol. 2021;62(7):966-978. <https://doi.org/10.1177/0284185120944916>
7. Meng XF, Zhu SC, Sun SJ, Guo JC, Wang X. Diffusion-weighted imaging for differential Diagnosis of benign vs malignant ovarian neoplasms: meta-analysis. Oncol Lett. 2016;11:3795-3802. <https://doi.org/10.3892/ol.2016.4445>
8. Zhang Q, Dai X, Li W. Systematic review and meta-analysis of O-RADS US and O-RADS MRI for ovarian/adnexal lesions. AJR Am J Roentgenol. 2023;221(1):21-33. <https://doi.org/10.2214/AJR.22.28396>
9. Moradi B, et al. Unenhanced MRI for indeterminate ovarian/adnexal masses: diagnostic accuracy study. Radiol Bras. 2025;58(1): ePub ahead of print. <https://doi.org/10.1590/0100-3984.2024.0032>
10. Pereira PN, Yoshida A, Sarian LO, et al. Accuracy of the ADNEX MR scoring system based on a simplified MRI protocol for the assessment of adnexal masses. Diagn Interv Radiol. 2018;24(2):63-71. <https://doi.org/10.5152/dir.2018.17378>
11. Hricak H, Chen M, Coakley FV, et al. Complex adnexal masses: detection and characterization with MR imaging—multivariate analysis. Radiology. 2000;214(1):39-46. <https://doi.org/10.1148/radiology.214.1.39>
12. Sohaib SAA, Sahdev A, Van Trappen P, Jacobs IJ, Reznek RH. Characterization of adnexal mass lesions on MR imaging. AJR Am J Roentgenol. 2003;180(5):1297-1304. <https://doi.org/10.2214/ajr.180.5.1801297>
13. Saini A, Dina R, McIndoe GA, Soutter WP, Gishen P, deSouza NM. Characterization of adnexal masses with MRI. AJR Am J Roentgenol. 2005;184(3):1004-1009. <https://doi.org/10.2214/ajr.184.3.01841004>
14. Kinkel K, Lu Y, Mehdizade A, Pelte MF, Hricak H. Indeterminate ovarian mass at US: incremental value of second imaging test for characterization—meta-analysis and Bayesian analysis. Radiology. 2005;236(1):85-94. <https://doi.org/10.1148/radiol.2361041618>
15. Taylor EC, Irshaid L, Mathur M. Multimodality imaging approach to ovarian neoplasms: state of the art. RadioGraphics. 2021;41(1):289-315. <https://doi.org/10.1148/rg.2021200086>
16. Derlatka P, Walecka A, Walecki J. The value of magnetic resonance diffusion-weighted imaging and dynamic contrast enhancement in the Diagnosis and prognosis of treatment response in patients with epithelial serous ovarian cancer. Cancers (Basel). 2022;14(10):2464. <https://doi.org/10.3390/cancers14102464>
17. Manganaro L, Micco M, Fagotti A, et al. Impact of DWI and ADC values in the O-RADS MRI classification for adnexal masses. Radiol Med. 2023;128(5):565-577. <https://doi.org/10.1007/s11547-023-01628-3>
18. Van Calster B, Van Hoorde K, Valentin L, et al. Evaluating the risk of ovarian cancer before surgery using the ADNEX model. BMJ. 2014;349:g5920. <https://doi.org/10.1136/bmj.g5920>
19. Van Calster B, Wynants L, Timmerman D, et al. Validation of models to diagnose ovarian cancer in patients with adnexal masses. BMJ. 2020;370:m2614. <https://doi.org/10.1136/bmj.m2614>
20. Sahin H, Panico C, Pacelli R, et al. Serous borderline ovarian tumours: an extensive review on MR imaging features. Br J Radiol. 2021;94(1125):20210116. <https://doi.org/10.1259/bjr.20210116>
21. Torre LA, Trabert B, DeSantis CE, et al. Ovarian cancer statistics, 2018. CA Cancer J Clin. 2018;68(4):284-296. <https://doi.org/10.3322/caac.21456>



**Open Access** This article is licensed under a Creative Commons Attribution 4.0 International License, <http://creativecommons.org/licenses/by/4.0/>. © The Author(s) 2025